Medical Image Analysis 18 (2014) 1329–1336

Contents lists available at ScienceDirect

Medical Image Analysis

journal homepage: www.elsevier.com/locate/media

Mini gamma cameras for intra-operative nuclear tomographic reconstruction

Philipp Matthies [a,*,1], José Gardiazabal [a,b,1], Aslı Okur [a,b], Jakob Vogel [a], Tobias Lasser [a], Nassir Navab [a]

[a] Computer Aided Medical Procedures (CAMP), Technische Universität München, Boltzmannstraße 3, 85748 Garching b. München, Germany
[b] Department of Nuclear Medicine, Klinikum Rechts der Isar, Technische Universität München, Ismaninger Straße 22, 81675 München, Germany

ARTICLE INFO

Article history:
Received 6 January 2014
Received in revised form 18 March 2014
Accepted 10 April 2014
Available online 26 April 2014

Keywords:
Image reconstruction (iterative)
Nuclear imaging
Intra-operative imaging

ABSTRACT

Nuclear imaging modalities like PET or SPECT are in extensive use in medical diagnostics. In a move towards personalized therapy, we present a flexible nuclear tomographic imaging system to enable intra-operative SPECT-like 3D imaging. The system consists of a miniaturized gamma camera mounted on a robot arm for flexible positioning, while spatio-temporal localization is provided by an optical tracking system. To facilitate statistical tomographic reconstruction of the radiotracer distribution using a maximum likelihood approach, a precise model of the mini gamma camera is generated by measurements. The entire system is evaluated in a series of experiments using a hot spot phantom, with a focus on criteria relevant for the intra-operative workflow, namely the number of required imaging positions as well as the required imaging time. The results show that high quality reconstructed images of simple hot spot configurations with positional errors of less than one millimeter are possible within acquisition times as short as 15 s.

© 2014 Elsevier B.V. All rights reserved.

1. Introduction

Originally developed several decades ago, advanced 3D anatomical and functional imaging modalities like CT, MRI, PET or SPECT play a crucial role in today's healthcare. Respective data sets are acquired routinely in clinical practice, providing accurate, patient-specific information for diagnosis and treatment planning. However, in their standard configuration, the respective scanners are very bulky, limiting their use in crowded intervention scenarios. This is particularly true for the nuclear imaging modalities, as considerable scanning time is required to obtain statistically significant measurements while still allowing for low radiation doses. Therefore, surgeons need to rely on – potentially outdated – pre-operative information during their work.

In the recent years, considerable efforts have been made to build devices for intra-operative imaging, thus enabling accurate guidance and quality assurance in the operating theatre. Important examples are 3D ultrasound and C-arm CT. Both modalities are successfully used in clinical practice, as shown, for instance, by Fenster and Downey (2000) and Ganguly et al. (2011).

In terms of nuclear imaging, Wendler et al. (2007) have introduced an intra-operative technique called "Freehand SPECT" (fhSPECT), and presented a first clinical setup (Wendler et al., 2010). Like its classical, diagnostic counterpart, fhSPECT relies on a radioactive tracer specifically targeting certain types of tissue, for example cancer cells. In some of the typical clinical scenarios, this radioactive tracer is already injected for pre-operative diagnostics, such as scintigraphy, and can be reused intra-operatively, adding no additional radiation dose, assuming the treatment follows sufficiently close to the diagnosis. Using a tracked detector for radioactivity, radiation values from known, well-distributed perspectives are acquired and reconstructed using tomographic solution techniques. Based on such three-dimensional activity maps, interesting hot spots can then be identified and localized interventionally. Currently, fhSPECT is used in sentinel lymph node biopsy for breast cancer (Bluemel et al., 2013), for melanoma (Rieger et al., 2011; Naji et al., 2011), for oral cancer (Heuveling et al., 2012), and in parathyroidectomy (Rahbar et al., 2012).

Unfortunately, fhSPECT reconstructions are of a considerably reduced quality in comparison to pre-operative SPECT, due to the short time of scanning (typically 2–5 min) using only a single detector. Consequently, the number of measurements is very small in comparison to the desired resolution of the images, thus limiting the quality and incurring artifacts (Wendler et al., 2010).

* Corresponding author. Tel.: +49 8928919401.
E-mail addresses: matthies@in.tum.de (P. Matthies), gardiaza@in.tum.de (J. Gardiazabal).
[1] The two authors contributed equally to the manuscript.

http://dx.doi.org/10.1016/j.media.2014.04.009
1361-8415/© 2014 Elsevier B.V. All rights reserved.

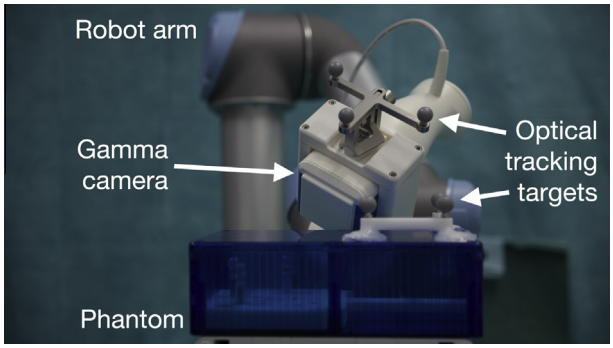

Fig. 1. Setup with optically tracked gamma camera attached to robot arm, scanning the likewise tracked phantom.

In order to address this problem, we have recently introduced newly developed, miniaturized gamma cameras for intra-operative nuclear tomographic imaging (Matthies et al., 2013). Using a mini gamma camera with 256 detector pixels held by a robot arm, we have shown tremendously improved intra-operative SPECT-like reconstructions compared to acquisitions using only a single detector.

In this paper, we elaborate on this earlier work, in particular addressing the question of how to trade off scanning time, number of scanned positions and angular coverage of the volume of interest versus image quality. Using an improved detection model of the mini gamma camera, we conduct a series of experiments on a hot spot phantom, showing that high accuracy can be reached reproducibly with radically shortened acquisition times.

2. Methods

The imaging setup consists of three parts: the mini gamma camera, the robot arm and the optical tracking system, see Fig. 1. The mini gamma camera acquires the gamma radiation from the nuclear tracer, the robot arm is used for moving the gamma camera, while the optical tracking system is used for spatial localization of the mini gamma camera in relation to the object to be imaged (in our case a hot spot phantom). The choice of the robot arm and the optical tracking for positioning and localization of the mini gamma camera is not critical for this work. In fact, any other, reasonably accurate and repeatable method would work as well, see also Section 4.2.

In the following, we describe the methods to connect these three parts together to enable nuclear tomographic reconstruction.

2.1. Measurements

The robot arm moves the camera to multiple measurement *poses* $\mathbf{y}_k = (\mathbf{p}_k, \mathbf{o}_k) \in \mathbb{R}^3 \times \mathbb{R}^3$ (that is *positions* $\mathbf{p}_k$ and *orientations* $\mathbf{o}_k$) distributed around a *volume of interest* $V \subset \mathbb{R}^3$. Simultaneously, the camera acquires 16×16 *detector readings* $m_j \geqslant 0$ as photon counts per second (cps), using a fixed *exposure time interval* denoted as t_{exp}. We use the unique index[2] j to refer to such a *single* detector reading, and the respective measured value is denoted as m_j.

The number k of measurement poses as well as their distribution in relation to the activity to be reconstructed is of very high importance to the quality of the images. Due to the expected constraints in time and space in intra-operative settings, the measurement poses will be very limited in number as well as sparsely distributed.

[2] A trivial bijective mapping is given by $j = k \cdot 256 + p$ where k denotes the pose index, and p a detector index in the camera pixel array.

2.2. Statistical tomographic reconstruction

The aim of the imaging setup is to recover the *radio*activity distribution $f : V \subset \mathbb{R}^3 \to [0, \infty)$. Its non-negative value describes the amount of radioactivity per location, for example the tracer uptake estimating the presence of cancer cells. We discretize this still unknown function f as

$$f(\cdot) \approx \hat{f}(\cdot) = \sum_i x_i b_i(\cdot), \tag{1}$$

where $b_i : V \to [0, \infty)$ denotes a user-defined voxel basis of V, and $\mathbf{x} = (x_i) \in \mathbb{R}^n$ denotes the vector of unknown coefficients. Once $\mathbf{x}$ is estimated from the measurements, the synthesis operator (1) will yield the approximated activity signal $\hat{f}$. For simplicity, we just use the index i to refer to voxel b_i.

The process of detector j detecting emissions from voxel i is modeled using a Poisson process, denoting the detection probability as

$$p(i,j) = P[\text{detected in } j \mid \text{emitted from } i]. \tag{2}$$

The detector readings m_j are thus interpreted as independently distributed Poisson random variables, with expectation

$$E(m_j) = \sum_i x_i \cdot p(i,j).$$

For tomographic reconstruction, we estimate $\mathbf{x}$ from the measurements $\mathbf{m}$ using a maximum likelihood estimator,

$$\arg\max_{\mathbf{x}} L(\mathbf{x}|\mathbf{m}),$$

with the log-likelihood

$$L(\mathbf{x}|\mathbf{m}) = m_j \log\left(\sum_i x_i \cdot p(i,j)\right) - \sum_i x_i \cdot p(i,j).$$

An approximated solution is computed iteratively using the maximum likelihood expectation maximization method (MLEM) by Shepp and Vardi (1982), that is for iteration index $q \in \mathbb{N}$ and all components $i \in \{1, \ldots, n\}$

$$x_i^{q+1} = x_i^q \cdot \frac{1}{\sum_j p(i,j)} \sum_j \frac{m_j \cdot p(i,j)}{\sum_i x_i \cdot p(i,j)},$$

with an initial value of $\mathbf{x}^0 = \mathbf{1} \in \mathbb{R}^n$.

2.3. Modeling of the mini gamma camera

A crucial component of the reconstruction process is knowledge of the detection probabilities $p(i,j)$ from Eq. (2), also denoted as the model of the mini gamma camera. While there are several ways of estimating the $p(i,j)$, in this work we measure an approximation in a calibration step by directly recording the detector response to a point source, see Section 2.3.1. An alternative approach is for example followed by Shakir et al. (2012), where the detector is modeled based on its geometry and the detection probabilities are calculated analytically. Another alternative is to compute the $p(i,j)$ using Monte Carlo simulations (Rafecas et al., 2004), which is computationally complex. The chosen method of direct measurement has the advantage that the exact geometry of the camera does not have to be known, and that it accounts for any errors in the setup, for example a misaligned collimator with respect to the camera pixels.

As the camera measurement poses $\mathbf{y}_k$ (resulting in the detector readings j) are arbitrary, and the discretization of the volume of

Download English Version:

https://daneshyari.com/en/article/444050

Download Persian Version:

https://daneshyari.com/article/444050

Daneshyari.com